



HAL
open science

Hydrophobic Tungsten-Containing MFI-Type Zeolite Films for Exhaust Gas Detection

Julien Grand, Siddulu Naidu Talapaneni, Hristiyan A. Aleksandrov, Georgi N.
Vayssilov, Svetlana Mintova

► **To cite this version:**

Julien Grand, Siddulu Naidu Talapaneni, Hristiyan A. Aleksandrov, Georgi N. Vayssilov, Svetlana Mintova. Hydrophobic Tungsten-Containing MFI-Type Zeolite Films for Exhaust Gas Detection. ACS Applied Materials & Interfaces, 2019, 11 (13), pp.12914-12919. 10.1021/acsami.8b17626 . hal-03027966

HAL Id: hal-03027966

<https://normandie-univ.hal.science/hal-03027966>

Submitted on 27 Nov 2020

HAL is a multi-disciplinary open access archive for the deposit and dissemination of scientific research documents, whether they are published or not. The documents may come from teaching and research institutions in France or abroad, or from public or private research centers.

L'archive ouverte pluridisciplinaire **HAL**, est destinée au dépôt et à la diffusion de documents scientifiques de niveau recherche, publiés ou non, émanant des établissements d'enseignement et de recherche français ou étrangers, des laboratoires publics ou privés.

Hydrophobic Tungsten Containing MFI-type Zeolite Films for Exhaust Gas Detection

Julien Grand,[†] Siddulu Naidu Talapaneni,[†] Hristiyan A. Aleksandrov,[§] Georgi N. Vayssilov[§] and Svetlana Mintova^{†,}*

[†]Laboratoire Catalyse et Spectrochimie (LCS), Normandie Univ, ENSICAEN, UNICAEN, CNRS, 16000 Caen, France.

[§]Faculty of Chemistry and Pharmacy, University of Sofia, 1126 Sofia, Bulgaria.

KEYWORDS

Zeolites nanocrystals, adsorption, thin films, IR spectroscopy, hydrophobicity, exhaust gas

ABSTRACT

The assembly of highly hydrophobic nanosized tungsten containing MFI type zeolite nanocrystals (W-MFI) in films, and their further use for selective exhaust gas (CO, CO₂, NO and NO₂) detection was investigated by operando IR spectroscopy. Due to the hydrophobic nature and the presence of tungsten in the framework, the W-MFI films showed excellent sorption capacity towards all analytes, in comparison to the pure silica (Si-MFI) film. The high sensitivity of the W-MFI film towards low concentration of CO₂ and NO₂ (1-3 ppm) was demonstrated. In addition, the interactions between the analytes and zeolite films have been studied by quantum chemical calculations modeling of the W centers based on the density functional theory method.

1. Introduction

The ingrowing demand of environmental sensing data urges the development of selective chemical sensors. Over the past decades, there is an increasing demand for the fabrication of highly efficient sensors that are able selectively to detect CO, CO₂ and NO_x pollutant gases at ppm levels, which are continuously produced from combustion engines.^{1,2} Issues concerned for the manufacturing of these type of sensors include materials sensitivity, selectivity, reproducibility, reliability, long-term stability and applicability to in-situ and real time measurements.³ Moreover, these functionalities of the sensors should be preserved in the harsh environment conditions including high temperature, variation of humidity, variation of temperature, pressure and concentration of highly acidic compounds that are common for automotive exhausts.

Microporous molecular sieves have been widely considered for selective sensor applications due to their well-defined pore structure, particle dimensions and morphology in line with high surface area, sorption capacity and catalytic activity.^{4,5} However, the slow diffusion of the analytes in the micropores of the micrometer-sized molecular sieves is not in *ad equation* with the real-time response requirements. Nanosized zeolites have been designed and prepared to leave behind these challenges. Variety of zeolite nanostructures and diverse depositing techniques on various supports were reported.⁶⁻⁸ As active layer of sensor devices, zeolite nanocrystals assembled as films are very favorable due to their high thermal stability, chemical resistance, enhanced specific surface area and decreased diffusion path lengths which leads to more sensitive tracking and real-time response to emissions.⁴ They can be deposited in thin-to-thick films using different approaches such as direct crystallization, seed growth, spin- and dip-coating, and sol-gel technique. The film thicknesses also influence the sorption capacity and diffusion rate, while the main features of zeolite nanocrystals (hydrophobicity, adsorptive properties and their interaction with the analytes)

determine their application for various sensors. Further properties have been improved by the confinement of desired metal clusters in the nanosized zeolite matrix.⁹⁻¹¹ However, the size and location control, as well as the hydrophilic nature of the clusters seem to be difficult to handle.^{12,13} Aluminum free zeolites, namely metallosilicates, have been widely considered to overcome these issues.¹⁴⁻¹⁶

Among the application of different metal oxides, the tungsten oxides have been found to be promising for the detection of NO_x gases.¹⁷⁻¹⁹ Although small sized tungsten oxide based materials display high sensitivities toward NO_x, the greatest limitation is due to their poor selectivity. Several groups showed that the selectivity for CO and NO_x gases by tungsten oxide can be improved by modification with porous silicon supports.²⁰ Very recently, our group has demonstrated a novel approach for the incorporation of tungsten in the framework of MFI-type zeolite affording silanol-free nanocrystals, which are highly hydrophobic in nature.^{21,22} Thus, the incorporation of tungsten in the nanosized zeolite framework is expected not only to provide materials with enhanced sensitivity toward exhaust gas but also to improve their hydrophobicity and thus their sorption capacity, as competition towards water sorption will be avoided.

Herein, we describe the preparation of tungsten containing MFI type zeolite nanocrystals (W-MFI) assembled in thin-to-thick films (600-1600 nm). The influence of the metal doping, the hydrophobicity and the film thicknesses on their performance for the selective detection of exhaust such as carbon monoxide, carbon dioxide, nitrogen oxide and nitrogen dioxide in the presence of water has been evaluated.

2. Experimental part

Preparation of W–MFI and Si–MFI zeolite coating suspensions

The stable coating suspensions of discrete nanosized W-MFI and Si-MFI type zeolites were prepared from colloidal precursors under hydrothermal synthesis conditions.²¹ The as-prepared precursor suspensions for W-MFI and Si-MFI zeolites were aged at room temperature for 24 h prior further hydrothermal treatment at 90 °C for 12 h. After the hydrothermal treatment, the zeolite nanoparticles were purified by three steps centrifugation (20000 rpm, 30 min) using distilled water and finally stabilized in coating suspension with a solid content of 1 wt. % using absolute ethanol (99.9 %, Aldrich) as a solvent.

Zeolite thin films assembly

The crystalline MFI type nanosized zeolites were assembled in thin films on silicon wafers by spin-on process. The silicon wafers (100) with a dimension of 10 × 10 mm² were pre-cleaned with ethanol and acetone and dried with air gun prior deposition of the films. The MFI coating suspensions with a solid content of 1 wt. % in ethanol were filtrated through syringe filters (450 nm). The procedure involves: (i) deposition of a smooth layer consisting of 5 wt. % polyvinylpyrrolidone (PVP, average molecular weight ~ 10000, Sigma-Aldrich) in absolute ethanol by spin coating (acceleration: 2000 rpm s⁻¹, 3000 rpm for 20 s) (Supporting Information, SI Figure S1), followed by (ii) deposition of one or several MFI zeolite layers by spin coating (acceleration: 2000 rpm s⁻¹, 500-3000 rpm for 20 s). After each coating step, the films were dried at 80 °C for 20 min in order to improve the mechanical stability. Variation of the spin-coating speed and the number of layers afforded films of various thicknesses (600-1600 nm). The films were calcined at 550 °C for 2 h to remove the binder layer (PVP) and the template used in the MFI zeolite synthesis process (tetrapropylammonium hydroxide, TPAOH). Finally, the W-MFI and Si-MFI films of 600 nm (sample W-MFI-600) and 1600 nm (sample W-MFI-1600) thicknesses were used for detection of exhaust gases.

Characterization of zeolites films

The zeolite nanoparticles as Si-MFI and W-MFI powders were fully described in a previous paper.²¹ The results from nitrogen sorption measurements of both materials are presented in Table S1 (see SI). The homogeneity features and thicknesses of the prepared MFI-type films were monitored by a field emission scanning electron microscope (FE-SEM TESCAN Mira). The crystalline structure of the films was studied with X-ray diffraction (XRD) using a PANalytical X'Pert Pro diffractometer in Debye-Scherrer geometry with Cu K α radiation ($\lambda = 1.5418 \text{ \AA}$). The thermal stability of the PVP binder was measured by thermogravimetric analysis (TGA) using a SETSYS evolution instrument; measurements in air atmosphere with a ramp heating of 5° C/min were carried out.

Detection of CO, CO₂, NO and NO₂: *operando* IR study

The detection of CO, CO₂, NO and NO₂ with zeolite films was followed by *operando* IR spectroscopy using a reactor cell and a gas flow system described in a previous paper.¹¹ The experiments were performed at 25° C under Argon (Ar) flow and atmospheric pressure. Prior measurements, the zeolite films were activated at 300° C for 6 h (ramping heating of 1° C/min) under Ar with a flow of $20 \text{ cm}^3/\text{min}$. The analytes (CO, CO₂, NO and NO₂) with a concentration ranging from 1 to 100 ppm in Ar with a total flow of $20 \text{ cm}^3/\text{min}$ were sent to the IR reactor cell. All experiments were performed in the presence of water with a concentration of 100 ppm coming from the Ar carrier gas. The IR spectra were collected in a continuous mode (32 scans/spectrum) with a Bruker Tensor 27 spectrometer equipped with a DTGS detector. The first spectrum was recorded after 30 seconds; the waiting time between each scan was 1 minute. After the measurements, the zeolite films were regenerated following the activation process described

above. The entire process including activation of samples (removal of adsorbed water and contaminants at 300 °C) and controlled adsorption and desorption of pure analytes (CO, CO₂, NO and NO₂) in subsequent cycles were performed in the *operando* IR cell in order to ensure identical conditions for the measurements.

Modeling of CO, CO₂, NO and NO₂ adsorption on W-MFI zeolite

Quantum chemical calculations based on the density functional theory method were carried out using periodic plane wave basis for the valence electrons with a cutoff energy of 400 eV. The calculations were performed with the Vienna *ab initio* simulation package (VASP)^{23,24} using the gradient corrected PW91 exchange-correlation functional²⁵ and ultrasoft pseudopotentials.^{26,27} The large size of the unit cell (see below) allowed us to sample the Brillouin zone using only the Γ point.²⁸ An orthorhombic unit cell of the MFI type zeolite framework was employed, which consists of 96 T atoms with dimensions: $a = 20.271 \text{ \AA}$, $b = 19.925 \text{ \AA}$, and $c = 13.332 \text{ \AA}$.²⁹ During the geometry optimization, all atoms of MFI structure as well as the adsorbate species were allowed to relax until the force on each atom becomes less than $2 \times 10^{-4} \text{ eV/pm}$. The vibrational frequencies of the CO and CO₂ adsorbate species were simulated and compared with the experimental data. They were calculated via a numerical normal mode analysis in which the Hessian elements were approximated as finite differences of analytical gradients, displacing each atomic center by 1.5 pm either way along each Cartesian direction.

3. Results and discussion

General characterization of zeolite powders and films

The W-MFI zeolite crystals used herein are silanol-free and hydrophobic (See SI, Figure S2 and previous work²¹) in nature meaning that no silanol groups are present and thus guarantee the film stability. Therefore, to ensure the preparation of smooth and homogeneous films with high mechanical stability, a polymeric PVP binder was used as first layer deposited on the pre-cleaned silicon wafers. Previously, the PVP has been used as wetting agent for the preparation of metal oxides thin films and nanowires without influencing their structure and morphology.³⁰ Moreover, the PVP was reported for efficient preparation of crack-free TiO₂ films having improved activity after PVP burnout.³¹ Therefore a thin PVP layer was used as a binder between the silicon wafer and the zeolite nanocrystals by enhancing their polar interactions and improving the wetting effect at the silicon wafer surface (Figure 1a). The PVP was easily removed during the calcination process at 550 °C as the TGA defines its decomposition at 425 °C (See SI, Figure S3). The nanosized zeolite crystals (Si-MFI and W-MFI) dispersed in ethanol were deposited on silicon wafers by spin coating method. The homogeneity and thickness of the Si-MFI and W-MFI films were confirmed by FE-SEM as shown in Figure 1.

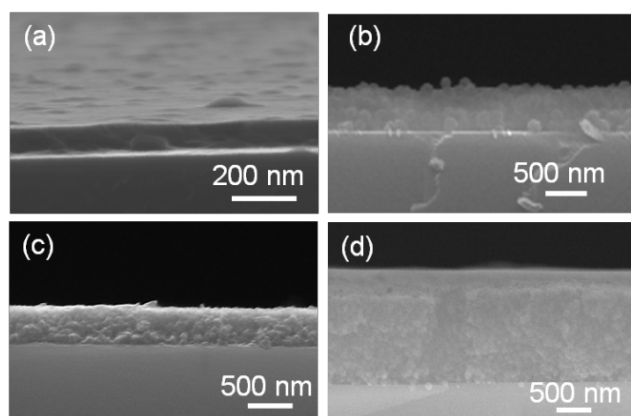


Figure 1. FE-SEM side-view images of (a) as-deposited PVP binder layer (100 nm), (b) calcined Si-MFI film (600 nm), (c) calcined W-MFI-600 film (600 nm) and (d) calcined W-MFI-1600 films (1600 nm).

Variation of the spin-coating speed and the number of layers afforded films of various thicknesses. After calcination, well-packed zeolite nanocrystals in the films covering entirely and homogeneously the silicon wafers were obtained. Si-MFI deposited as a reference thin film has been prepared comparable with the W-MFI one (Figure 1b and 1c). The highest thickness holding an homogeneous and stable zeolite film has been measured as 1.6 μm (Figure 1d). No traces of the PVP were observed after calcination (See SI, Figure S4). In addition, the X-ray diffraction pattern showed the high crystallinity and purity of the MFI nanocrystals assembled in the films (See SI, Figure S5). The XRD pattern for the thicker film was analogous to the corresponding pattern recorded from the MFI powder sample with random crystal orientation; the peak at $33^\circ 2\theta$ corresponds to a signal of the silicon wafer.

In the following experiments, zeolite films with thicknesses of 600 nm (W-MFI-600) and 1600 nm (W-MFI-1600) have been used.

Water adsorption of zeolite powders and films

The water adsorption on both zeolite powders and films (W-MFI and Si-MFI) has been studied using TG and *operando* IR spectroscopy (Figure 2). As expected the W-MFI zeolite crystals without silanol groups exhibit high hydrophobicity (See SI, Figure S2 and previous work²¹).

Calcined Si-MFI and W-MFI powder samples were kept during 7 consecutive days at relative humidity (RH) of 70%. The total water adsorbed in the two samples has been evaluated using TG analysis (Figure 2a). It is clearly observed that even the pure silica zeolite (Si-MFI) contains about 4 % water. The weight loss below 150 °C corresponds to water adsorbed in the channels and on the surface of the Si-MFI zeolite. Moreover, with decreasing the size of the Si-MFI zeolite crystals, a substantial increase of the external surface area and silanol-defect sites are observed as shown by N₂ sorption and *in situ* IR studies (Figure S6).

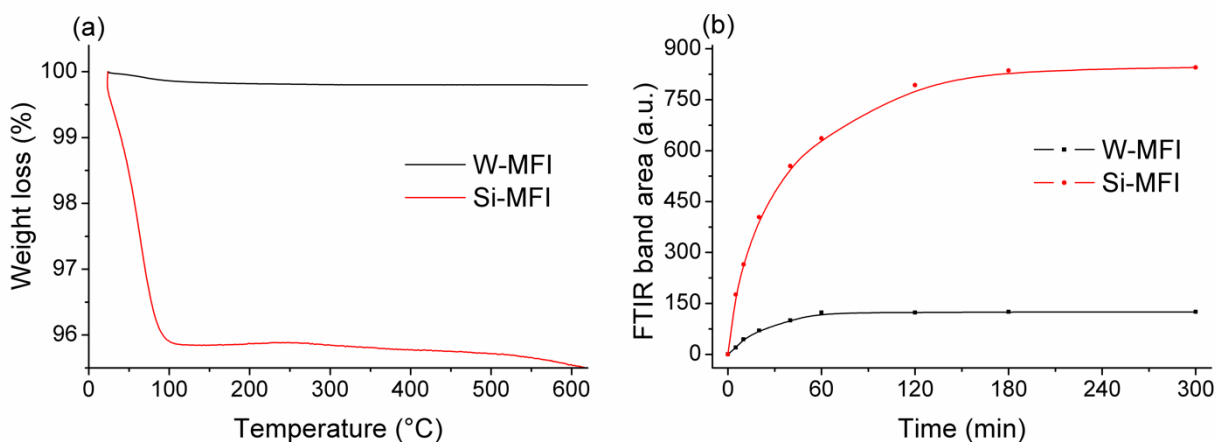


Figure 2. (a) Water content in calcined W-MFI (black) and Si-MFI (red) powder samples stored at 70% relative humidity (RH) after 7 days measured by TG and (b) water adsorption on activated W-MFI-1600 (black) and Si-MFI-1600 (red) films exposed to 100 ppm of water for 300 minutes monitored by *operando* FTIR spectroscopy (band area at 1600 cm⁻¹).

While the W-MFI zeolite shows less than 0.2 % weight loss, which is in the range of the measurement error (± 0.1 %). In parallel, the capacity of activated W-MFI-1600 and Si-MFI-1600 zeolite films (300 °C, 6 h) towards water vapor (100 ppm concentration in argon flow) was followed by *operando* IR spectroscopy (Figure 2b). The FTIR spectroscopy data is in agreement with the results obtained for zeolite powders (Figure 2a). The Si-MFI film absorbed 27 times more

water than the W-MFI film calculated from the bands areas at 3500 and 1600 cm^{-1} . Based on the above results, it is expected that the sensitivity towards the exhaust gases (NO , NO_2 , CO and CO_2) in the presence of water would not be disturbed in the case of the W-MFI films.

Effect of the film thickness on detection of NO and NO_2

The response of W-MFI zeolite films (W-MFI-600 and W-MFI-1600) toward low concentration of NO and NO_2 analytes (1-5 ppm) is depicted in Figure 3. Detailed kinetics data is provided in SI (Figures S7 and S8).

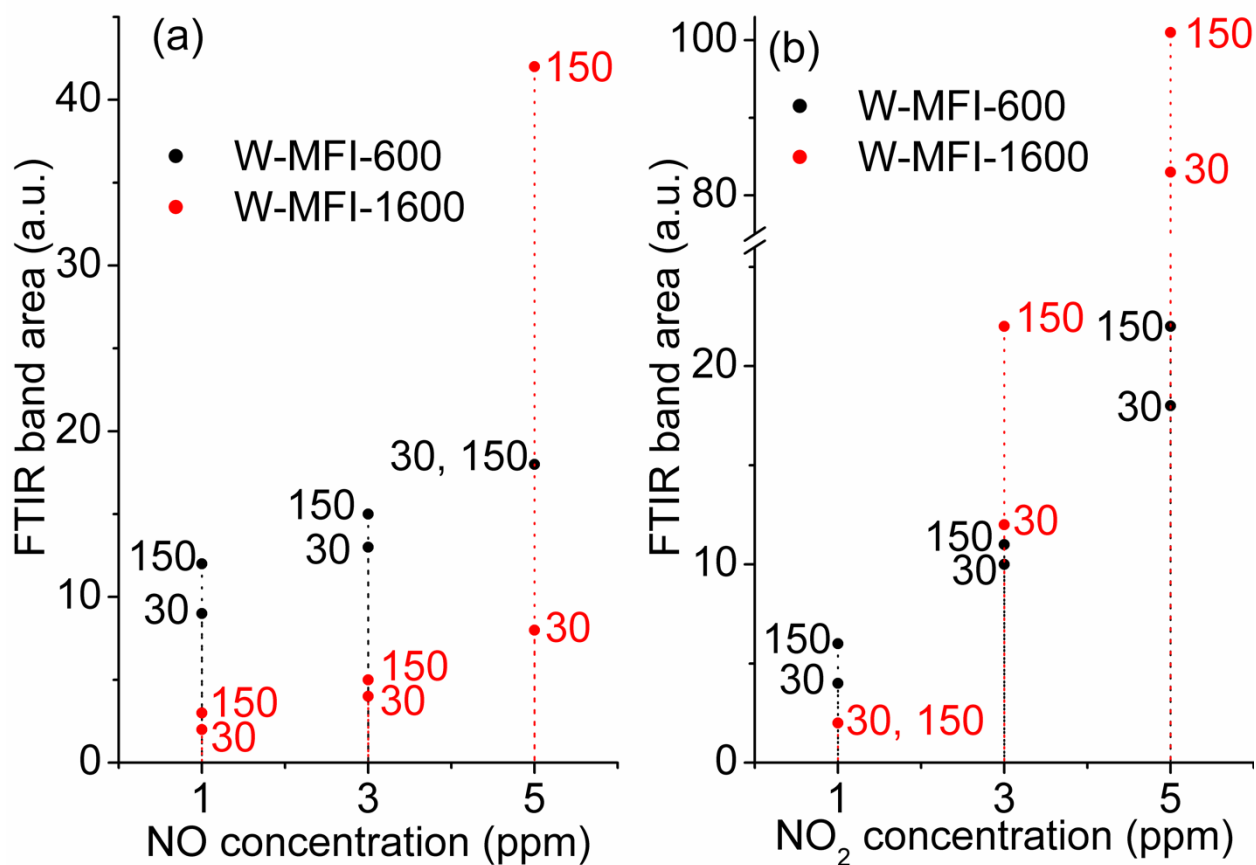


Figure 3. Responses of activated zeolite films W-MFI-600 (black) and W-MFI-1600 (red) exposed to (a) NO and (b) NO₂ gas (concentrations 1-5 ppm) in the presence of 100 ppm of water monitored by *operando* FTIR spectroscopy after 30 and 150 seconds.

As general trend, for both W-MFI zeolite films (W-MFI-600 and W-MFI-1600) the area of the IR bands in the range 1650 - 1480 cm⁻¹, corresponding to monodentate and bidentate nitrites/nitro compounds,^{32,33} increased with increasing of the analyte concentration and exposure time.

At low concentration (1 ppm), the W-MFI-600 film shows faster response in comparison to the W-MFI-1600 which is explained with faster diffusion in the thinner film. Indeed, both analytes (Figure 3) were effectively and distinctly detected by the W-MFI-600 film after 30 and 150 seconds. On the contrary, low responses were observed using the W-MFI-1600 film regardless of the time of exposure, meaning that 1 ppm concentration is too low to afford a reliable response using the W-MFI-1600 film.

At slightly higher concentration (3-5 ppm), both films exhibit clear response towards both analytes. However, at 5 ppm of NO, the responses after 30 and 150 seconds of the WMFI-600 film are mingled which means that the saturation appears in the first minute (Figure 3a). This phenomenon is not observed with the W-MFI-1600 film (Figure 3a). It appears that at 3 ppm NO₂, (Figure 3b) a remarkable increase in the response with the WMFI-1600 film with exposure time is observed. This film shows higher response compared to the one obtained with the WMFI-600 film. This implies that at concentration of analytes of 3-5 ppm, the sorption capacity overcomes the limiting low diffusion rate observed at 1 ppm. In addition, the low sensitivity of the thicker film is rapidly overcome by its high sorption capacity.

A similar trend has been observed when both films were exposed to CO and CO₂ analytes. The IR bands at 1380-1590 cm⁻¹ corresponding to chemisorbed carbonates and the one centered at 2290-2390 cm⁻¹ corresponding to physisorbed carbonates were measured (See SI Figures S9a and S9b). The W-MFI-1600 film shows high response towards analytes with a concentration of 3-5 ppm compared to the W-MFI-600 film. Therefore the W-MFI-1600 film was further used for the follow up experiments; the concentration of the analytes was increased up to 100 ppm.

Detection of exhaust gases using zeolite films: *operando* IR study

The detection of exhaust gases (NO, NO₂, CO and CO₂ with concentrations 1 - 100 ppm) in argon flow by W-MFI-1600 and Si-MFI-1600 films were followed by *operando* IR spectroscopy (SI, Figure S10). Spectra were recorded until a saturation at each concentration was reached. Importantly, all experiments were performed in the presence of water (100 ppm from the Ar flow) to prove that the enhanced hydrophobicity has a significant effect on sorption capacity and sensitivity of the zeolite films. The integrated IR bands at saturation level attributed to the adsorption of the corresponding species on the Si-MFI-1600 and W-MFI-1600 films are following a Langmuir type evolution with the increase of the analytes concentrations (Figure 4). The change of the IR bands in the range 1650 - 1480 cm⁻¹ for both NO and NO₂ analytes on W-MFI-1600 film, corresponding to monodentate and bidentate nitrites/nitro compounds,^{32,33} respectively are followed as a function of gas concentrations.

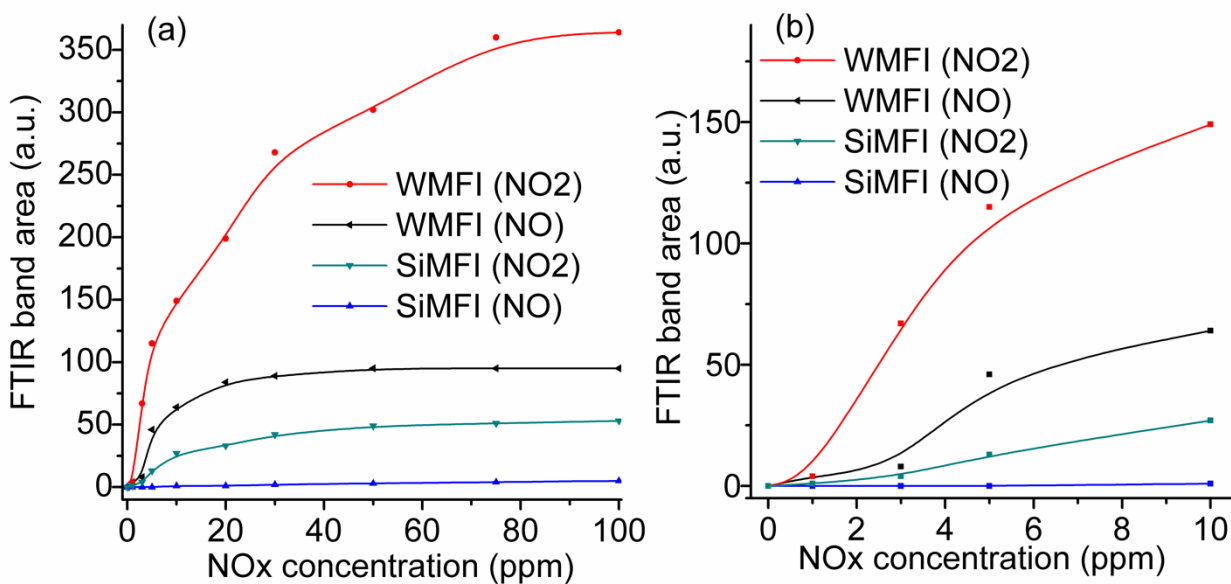


Figure 4. Detection of NO with W-MFI-1600 (black) and Si-MFI-1600 (blue), and NO₂ with W-MFI-1600 (red) and Si-MFI-1600 (green) films; IR band areas (1650 - 1480 cm⁻¹) are measured at concentrations (a) 1-100 ppm and (b) 1-10 ppm NO and NO₂.

The highest sensitivity of the W-MFI-1600 film towards NOx in comparison to the Si-MFI-1600 film is clearly demonstrated (Figure 4a). The Si-MFI-1600 film shows no readable response towards the NO analyte whereas the W-MFI-1600 reached its saturation level at 30 ppm. In addition, a clear response is observed at 5 ppm (Figure 4b). Concerning the NO₂ sorption, the saturation level is reached at around 30 ppm with Si-MFI-1600 film, while for the W-MFI-1600 film is higher than 75 ppm (Figure 4a).

The change of the IR bands at 1380-1590 cm⁻¹ corresponding to chemisorbed carbonates and the one centered at 2290-2390 cm⁻¹ corresponding to physisorbed carbonates are followed at different gas concentrations (Figure 5).³⁴ The data related to 1 ppm CO and CO₂ are not reported here since no readable responses were observed with both Si- and W-MFI films.

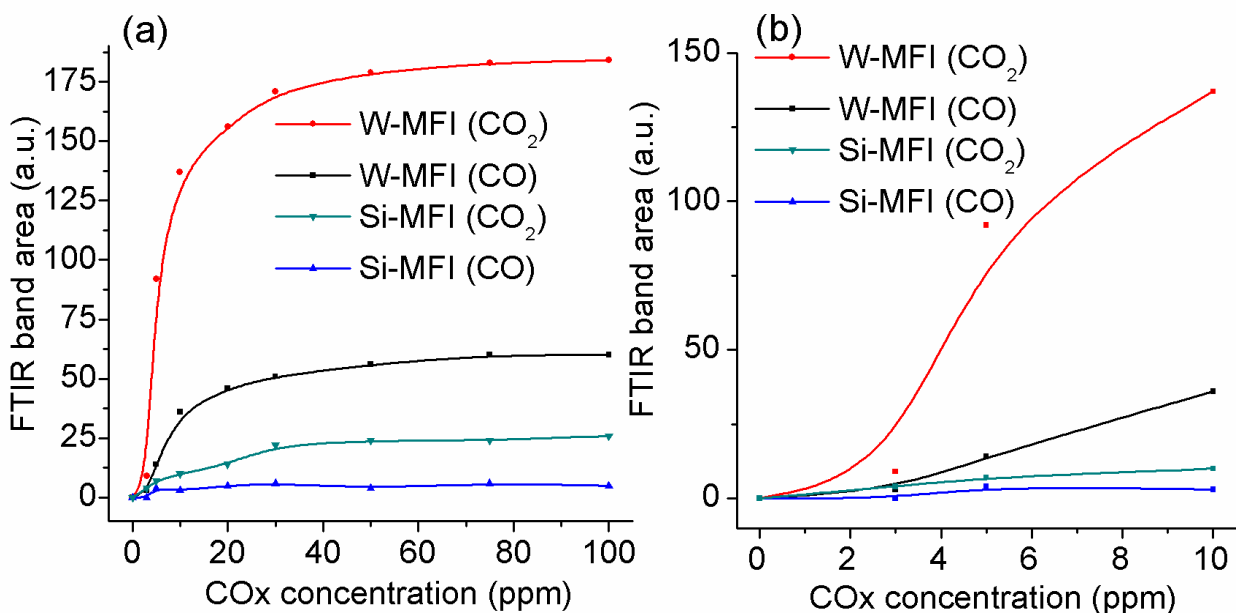


Figure 5. Detection of CO with W-MFI-1600 (black) and Si-MFI-1600 (blue) films and CO₂ with W-MFI-1600 (red) and Si-MFI-1600 (green) films following the evolution of the band areas corresponding to chemisorbed and physisorbed carbonates: (a) 3-100 ppm and (b) 3-20 ppm CO and CO₂, respectively.

The W-MFI-1600 film shows excellent selectivity and sensitivity toward CO₂ in comparison with the Si-MFI-1600 film and in comparison with the CO (Figure 5a). Indeed, the W-MFI-1600 film was saturated at higher concentrations (around 50 ppm) with both CO and CO₂ gas. Whereas the Si-MFI-1600 showed no clear response to CO in the concentrations range used, as well as no clear response for CO₂ (20-30 ppm) (Figure 5a). On the contrary, the first response of the W-MFI-1600 film at 3 ppm CO₂ and at 5-10 ppm CO were measured (Figure 5b).

Modeling of the NO, NO₂, CO and CO₂ adsorption on the W-MFI zeolite

The adsorption of NO, NO₂, CO and CO₂ analytes have been modeled on the most stable species W^{VI}=O which were found to exist in the W-MFI zeolite nanocrystals as reported in our previous work (Figure 6).²¹

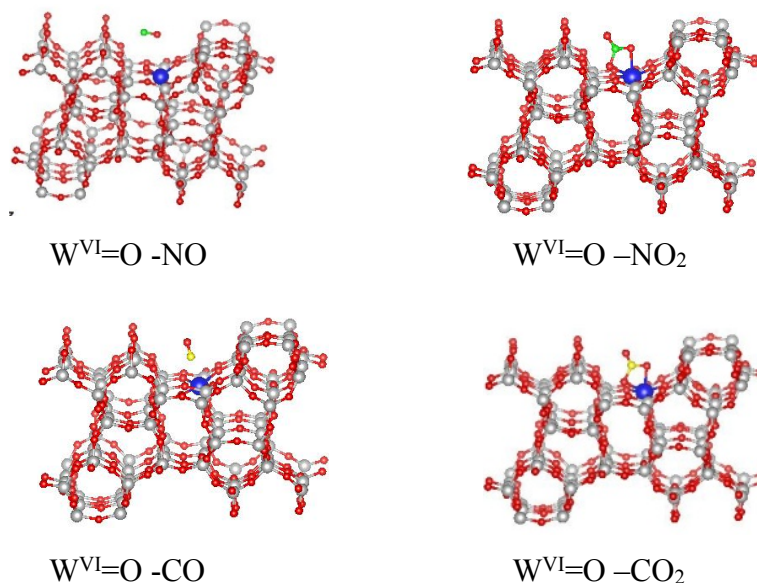


Figure 6. Optimized structures for NO, NO₂, CO and CO₂ adsorption at W^{VI}=O site of the W-MFI zeolite. In the cases of NO₂ and CO₂ adsorption corresponding nitrate (W^{VI}=O -NO₂) and carbonate (W^{VI}=O -CO₂) species are formed. Color coding: Si – grey, W – blue, O – red, N – green, C - yellow.

Adsorption of NO molecule to W^{VI}=O species in the W-MFI does not lead to the formation of adsorption complex as the guest molecule does not interact directly with the W^{VI}=O center. Concerning the NO₂ analyte, the formation of nitrate species was obtained when NO₂ is adsorbed by the W^{VI}=O center of the W-MFI zeolite. Its structure is bidentate, and the third oxygen center from the nitrate is not coordinated to a cationic center. Similarly to NO, CO molecule does not interact with W^{VI}=O species, while in the case of CO₂ adsorption carbonate species are formed at the W^{VI}=O moiety. In the obtained structure the carbonate is bound in bidentate fashion to the

tungsten and the third oxygen center from the carbonate is not coordinated to a cationic center. Using the notation of surface carbonates, introduced by Vayssilov et al.³⁵, those carbonate species can be assigned as 1.10 type. The theoretical results combined with the experimental clearly show that the introduction of a WO center in the zeolite framework has distinct effects on the improved sorption behavior of the W-MFI zeolite compared to the Si-MFI zeolite. Indeed, the formation of bidentate species, such nitrates or carbonates, is only favored by the $W^{VI}=O$ center, which is not present in the Si-MFI zeolite. Otherwise, when the analyte is monodentate (CO and NO), no interaction with the W center could be found. However, the sorption capacity is improved for the W-MFI. It means that the highly hydrophobic silanol-free structure obtained by the introduction of W has a positive effect on the sorption capacity of the MFI type zeolite. Indeed, the absence of water due to the absence of silanols in the W-MFI zeolite leads to an increase capacity for NO and CO analytes on the W-MFI zeolites. This non-competitive water/analytes sorption could be applied to every type of analytes different from water. The range and limitations of this phenomenon is under investigation.

Conclusions

The assembly of hydrophobic W-MFI and Si-MFI type zeolite nanocrystals in thin films for selective detection of exhaust gases (CO, CO₂, NO, NO_x) was carried out. The zeolite nanocrystals were spin-coated on silicon wafers using a polymer as a binder in order to increase the mechanical stability of the films. Besides, a multi-step deposition of the zeolite nanocrystals was applied to afford homogeneous films with thicknesses from 600 to 1600 nm with high thermal and mechanical stability. Zeolite films with a thickness 600 and 1600 nm films were further used for

detection of low concentrations of exhaust gases (1-100 ppm of CO, CO₂, NO and NO₂) in the presence of water (100 ppm).

The fastest detection of the exhaust gases was measured with the thinner film (600 nm), however, the thicker films (1600 nm) showed higher sorption capacity. The fast detection is explained with the fast diffusion within the thin films in comparison to the thick one. The saturation of the W-MFI zeolite films towards all analytes is reached after 2 minutes at 30 ppm concentration. High sensitivity of the W-MFI zeolite films compared to pure Si-MFI films towards very low concentrations (1-30 ppm) of exhaust gases in the presence of 100 ppm of water was demonstrated.

The highly hydrophobic nanosized zeolites with incorporated W in the framework (W-MFI) deposited in thin films demonstrate high molecular recognition capacity toward low concentrations of exhaust gases. It has been shown that the W-MFI films can detect low concentration of NO₂ and CO₂ (1-3 ppm). The highest sensitivity and sorption capacity of W-MFI film was observed towards NO₂ exposure (1 ppm).

ASSOCIATED CONTENT

Supporting information.

The supporting information file includes: Polyvinylpyrrolidone structure (Figure S1); Silanol-free zeolite nanocrystals evidenced by ²⁹Si NMR and FTIR spectroscopies (Figure S2); TG and dTG analysis of PVP polymer (Figure S3); PVP removal by calcination process evidenced by FTIR spectroscopy (Figure S4); XRD patterns of W-MFI zeolite as bulk and as thin film (Figure S5); N₂ sorption and FTIR spectra of nanosized and micronsized Si-MFI zeolites (Figure S6); Kinetic evolution of NO analyte adsorption on W-MFI films (Figure S7); Kinetic evolution of NO₂ analyte

adsorption on W-MFI films (Figure S8); Kinetic responses of W-MFI zeolite films exposed to CO and CO₂ gas (Figure S9).

AUTHOR INFORMATION

Corresponding author

*Email: Svetlana.mintova@ensicaen.fr

ACKNOWLEDGMENT

We acknowledge the financial support from the C²-MTM project « EMERGENTS » Region of Normandy and Marie Lozier for technical support. H.A.A. acknowledges financial support by the Bulgarian Science Fund (Project DFNI-T02/20).

REFERENCES

- (1) Wales, D. J.; Grand, J.; Ting, V. P.; Burke, R. D.; Edler, K. J.; Bowen, C. R.; Mintova, S.; Burrows, A. D.; Gas Sensing Using Porous Materials for Automotive Applications. *Chem. Soc. Rev.* **2015**, *44*, 4290-4321.
- (2) Wetchakun, K.; Samerjai, T.; Tamaekong, N.; Liewhira, C.; Siriwong, C.; Kruefu, V.; Wisitsoraat, A.; Tuantranont, A.; Phanichphant, S.; Semiconducting Metal Oxides as Sensors for Environmentally Hazardous Gases. *Sens. Actuat. B* **2011**, *160* (1), 580-591.
- (3) Liu, X.; Cheng, S.; Liu, H.; Hu, S.; Zhang, D.; Ning, H.; A Survey on Gas Sensing Technology. *Sensors* **2012**, *12* (7), 9635-9665.

- (4) Zheng, Y.; Li, X.; Dutta, P. K.; Exploitation of Unique Properties of Zeolites in the Development of Gas Sensors. *Sensors* **2012**, *12* (7), 5170-5194.
- (5) Korotcenkov, G.; Handbook for Gas Sensor Materials - Properties, Advantages and Shortcomings for Applications, Vol.2: New Trends And Technology, Springer, New-York, **2014**, 2.
- (6) Mintova, S.; Grand, J.; Valtchev, V.; Nanosized Zeolites: Quo Vadis ?. *C. R. Chim.* **2016**, *19* (1-2), 183-191.
- (7) Valtchev, V.; Tosheva, L.; Porous Nanosized Particles: Preparation, Properties, and Applications. *Chem. Rev.* **2013**, *113* (8), 6734-6780.
- (8) Naydenova, I.; Grand, J.; Mikulchyk, T.; Martin, S.; Toal, V.; Georgieva, V.; Thomas, S.; Mintova, S.; Hybrid Sensors Fabricated by Inkjet Printing and Holographic Patterning. *Chem. Mater.* **2015**, *27* (17), 6097-6101.
- (9) Talapaneni, S. N.; Grand, J.; Thomas, S.; Ahmed, H. A.; Mintova, S.; Nanosized Sn-MFI Zeolite for Selective Detection of Exhaust Gases. *Mater. Design* **2016**, *99*, 574-580.
- (10) Dubbe, A.; The Effect of Platinum Clusters in the Zeolite Micropores of a Zeolite-Based Potentiometric Hydrocarbon Gas Sensor. *Sens. Act. B* **2009**, *137* (1), 205-208.
- (11) Thomas, S.; Bazin, P.; Lakiss, L.; de Waele, V.; Mintova, S.; In Situ Infrared Molecular Detection Using Palladium-Containing Zeolite Films. *Langmuir* **2011**, *27* (7), 14689-14695.
- (12) Fukumura, H.; Irie, M.; Iwasawa, Y.; Masuhara, H.; Uosaki, K.; *Molecular Nano Dynamics*; Wiley-VCH: Weinheim, Germany, **2009**, 2.

- (13) Okumura, K.; Matsui, H.; Sanada, T.; Arao, M.; Honma, T.; Hirayama, S.; Niwa, M.; Generation of the Active Pd Cluster Catalyst in the Suzuki–Miyaura Reactions: Effect of the Activation with H₂ Studied by Means of Quick XAFS. *J. Catal.* **2009**, *265*, 89-98.
- (14) Blasco, T.; Cambor, M. A.; Corma, A.; Esteve, P.; Martinez, A.; Prieto, C.; Valencia, S.; Unseeded Synthesis of Al-Free Ti-B Zeolite in Fluoride Medium: A Hydrophobic Selective Oxidation Catalyst. *Chem. Commun.* **1996**, (20), 2367-2368.
- (15) Pinto, M. L.; Rocha, J.; Gomes, J. R. B.; Pires, J.; Slow Release of NO by Microporous Titanosilicate ETS-4. *J. Am. Chem. Soc.* **2011**, *133* (16), 6396-6402.
- (16) Corma, A.; Nemeth, L. T.; Renz, M.; Valencia, S.; Sn-zeolite Beta as a Heterogeneous Chemoselective Catalyst for Baeyer-Villiger Oxidations. *Nature* **2001**, *412* (6845), 423-425.
- (17) Kim, S.-J.; Hwang, I.-S.; Choi, J.-K.; Lee, J.-H.; Gas sensing characteristics of WO₃ nanoplates prepared by acidification method. *Thin Solid Films* **2011**, *519* (6), 2020-2024.
- (18) Qin, Y.; Hu, M.; Zhang, J.; Microstructure Characterization and NO₂-sensing Properties of Tungsten Oxide Nanostructures. *Sens. Act. B* **2010**, *150* (1), 339-345.
- (19) Varsani, P.; Afonja, A.; Williams, D. E.; Parkin, I.; Binions, R.; Zeolite-Modified WO₃ Gas Sensors – Enhanced detection of NO₂. *Sens. Act. B* **2011**, *160* (1), 475-482.
- (20) Yan, W.; Hu, M.; Zeng, P.; Ma, S.; Li, M.; Room Temperature NO₂-Sensing Properties of WO₃ Nanoparticles/Porous Silicon. *App. Surf. Sci.* **2014**, *292*, 551-555.

- (21) Grand, J.; Talapaneni, S. N.; Vicente, A.; Fernandez, C.; Dib, E.; Aleksandrov, H. A.; Vayssilov, G. N.; Retoux, R.; Boullay, P.; Gilson, J.-P.; Valtchev, V.; Mintova, S.; One-pot Synthesis of Silanol-free Nanosized MFI Zeolite. *Nature Mater.* **2017**, *16* (10), 1010-1016.
- (22) Mintova, S.; Talapaneni, S. N.; Grand, J.; Gilson, J. P.; Method for the Preparation of Defect-free Nanosized Synthetic Zeolite Materials. WO Pat., 2017068387A1, 2017.
- (23) Kresse, G.; Hafner, J.; Ab initio Molecular-Dynamics Simulation of the Liquid-Metal-Amorphous-Semiconductor Transition in Germanium. *J. Phys. Rev. B* **1994**, *49* (20), 14251-14269.
- (24) Kresse, G.; Furthmüller, J.; Efficiency of Ab-Initio Total Energy Calculations for Metals and Semiconductors Using a Plane-Wave Basis Set. *Comput. Mater. Sci.* **1996**, *6* (1), 15-50.
- (25) Perdew, J. P.; Wang, Y.; Accurate and Simple Analytic Representation of the Electron-Gas Correlation Energy. *Phys. Rev. B* **1992**, *45* (23), 13244-13249.
- (26) Vanderbilt, D.; Soft Self-Consistent Pseudopotentials an a Generalized Eigenvalue Formalism. *Phys. Rev. B* **1990**, *41* (11), 7892-7895.
- (27) Kresse, G.; Hafner, J.; Norm-Conserving and Ultrasoft Pseudopotentials for First-Row and Transition Elements. *J. Phys.: Condens. Matter.* **1994**, *6*, 8245-8257.
- (28) Jeanvoine, Y.; Angyan, J.; Kresse, G.; Hafner, J.; Brønsted Acid Sites in HSAPO-34 and Chabazite: An Ab Initio Structural Study. *J. Phys. Chem. B* **1998**, *102* (29), 5573-5580.
- (29) Baerlocher, C.; McCusker, L. B.; *Database of Zeolite Structures*. Available at: <http://www.iza-structure.org/databases>.

- (30) Enculescu, I.; Matei, E.; Sima, M.; Enculescu, M.; Sima, M.; Ghica, C.; Influence of Polyvinylpyrrolidone as an Additive in Electrochemical Preparation Of ZnO Nanowires and Nanostructured Thin Films. *Surf. Interface Anal.* **2008**, *40* (3-4), 556-560.
- (31) Tanaka, K.; Fukuyoshi, J.; Segawa, H.; Yoshida, K.; Improved Photocatalytic Activity of Zeolite- and Silica-Incorporated TiO₂ Film. *J. Hazard. Mater.* **2006**, *137* (2), 947-951.
- (32) Hadjiivanov, K.; Use of Overtones and Combination Modes for the Identification of Surface NO_x Anionic Species by IR Spectroscopy. *Catal. Lett.* **2000**, *68* (3-4), 157-161.
- (33) Hadjiivanov, K.; Identification of Neutral and Charged N_xO_y Surface Species by IR Spectroscopy. *Catal. Rev. Sci. Engin.* **2000**, *42* (1-2), 71-144.
- (34) Kock, E.-M.; Kogler, M.; Bielz, T.; Klotzer, B.; Penner, S.; In Situ FT-IR Spectroscopic Study of CO₂ and CO Adsorption on Y₂O₃, ZrO₂, and Ytria-Stabilized ZrO₂. *J. Phys. Chem. C* **2013**, *117* (34), 17666-17673.
- (35) Vayssilov, G. N.; Mihaylov, M.; Petkov, P. St.; Hadjiivanov, K. I.; Neyman, K. M.; Reassignment of the Vibrational Spectra of Carbonates, Formates, and Related Surface Species on Ceria: A Combined Density Functional and Infrared Spectroscopy Investigation. *J. Phys. Chem. C* **2011**, *115* (47), 23435-23454.